ACADEMY OF SCIENCES OF THE USSR

P. N. LEBEDEV PHYSICAL INSTITUTE

Preprint N 215

Laser Plasma Physics

Basov N.G., Volosevich P.P., Gamaly E.G., Gasilov V.A., Gus'kov S.Yu., Demchenko N.N., Zmitrenko N.V., Karpov V.Ya., Lebo I.G., Mishchenko T.V., Myshetskaya E.E., Rozanov V.B., Samarsky A.A., Tishkin V.F., Favorsky A.P.

COMPUTER SIMULATION OF HIGH ASPECT RATIO LASER PELLET IMPLOSION

Moscow - 1983

COMPUTER SIMULATION OF HIGH ASPECT RATIO LASER PELLET IMPLOSION

N.G.Basov, P.P.Volosevich*, E.G.Gamaly, V.A.Gasilov*, S.Yu. Gus'kov, N.N.Demchenko, N.V.Zmitrenko*, V.Ya.Karpov*, I.G.Lebo, T.V.Mishchenko*, E.E.Myshetskaya*, V.B.Rozanov, A.A.Samarsky*, V.T.Tishkin *, A.P.Favorsky *

P.N.Lebedev Physical Inst., USSR Acad.Sci., Moscow

* M.V.Keldysh Inst. of Applied Maths., USSR Acad.Sci., Moscow

1. The paper presents results of one- and two-dimensional simulations of high-aspect ratio ($A_S = \frac{R_s^o}{\Delta_s}$) gas-filled shells implosion (A_S of the order of some hundreds) under the nanosecond laser pulse.

The shell implosion velocity grows up with the aspect ratio increase under hydrodynamic regime of compression /1,2/. So, the use of thin shells in laser fusion experiments opens up the possibility to reach implosion velocities exceeding 200 km/sec needed for fu - sion reaction initiation.

The calculations have been performed for *1 kJ laser energy which corresponds to thin shell implosion experiments carried out at Delphin /3/ and Omega /4/ installations. Shell implosion velo - city, hydrodynamic efficiency, plasma density and temperature, thin shell implosion stability are discussed as functions of aspect ratio and the laser flux density.

2. Numerical calculations have been performed using "Luch","Diana" (1 -D) and "Atlant" (2-D) mathematical codes developed at Keldysh Institute of Applied Mathematics of the USSR Academy of Sciences

/5-7/. Codes include 1-D or 2-D hydrodynamic, electron and ion heat conduction, electron-ion relaxation, classical and anomalous laser light absorption, hot electron and radiation transport, ionization, fusion reactions, real equation of state and spontaneous magnetic field generation.

Numerical method is based on completely conservative additive finite difference schemes.

3. One-dimensional calculations have been performed for D_2-gas-filled shells. Fig.1 shows target and laser pulse parameters. To interprete 1-D simulation results the scaling from the analytical theory for compression and heating thin shell targets under the laser pulse has been used /1,2/.

Analytical theory assumes hydrodynamic (ablative) target implosion under ablative pressure calculated on the basis of stationary spherical corona with inverse bremstrahlung absorption and classical heat conductivity. Initial entropy is created by shock waves. The shock waves are followed by adiabatic compression.

Fig.2 presents implosion velocities u_s^* versus aspect ratio $A_s = R_s^\circ/\Delta_s$ from two series of numerical calculations for two flux density values. These functions are in good agreement with the analytical scaling $u_s^* \sim A_s^{1/2} \cdot q^{1/3}$. Implosion velocity 200 km/s is achieved at A_s=250 for q =1.8.10^{13} W/cm^2.

Fig.3 shows normalized ablated shell mass M_{ab}/M_s° and hydrodynamic efficiency η as function of aspect ratio for the same series of calculations. According to analytical theory the ablated mass value grows slower with the aspect ratio increase than the relation $\sim A_s^{1/2}$ implies. For A_s=150-400 calculated values are

M_{ℓ}/M_g°=50-75%, η =8-10%. The results confirm analytical theory important conclusion that maximal mass-averaged gas temperature saturates with aspect ratio increasing (Fig.4). For example at initial shell and gas densities ρ_s° =2.5 g/cm^3 and ρ_g° =10^{-3}g/cm^3, respectively, the temperature saturated at A_s=100.

Maximal gas density obtained in numerical calculations slowly varies with flux density, which disagrees with analytical theory predictions. However, on the whole, numerical calculation results confirm the theoretical predictions as to fast decrease of final gas density with aspect ratio growth: $\rho_g^{*} \sim A_s^{-1/\gamma-1}$ at sufficiently high A_s(Fig.5). For A_s>100-150 neutron yield increases with A_s decrease in accordance with effect of temperature saturation and final gas density decrease when A_s increases. For example, N=1.5.10^8 at A_s=133 and q =1.2.10^{13}W/cm^2. In the experiments /3/absorbed energy was E_{abs}=400-600 J, targets with initial radius R=200 - 300 μm and aspect ratio A_s=150-250. Average implosion velocities of 160-180 km/s and volume compression of order 10^3 were measured under laser pulse duration τ_L =2.3 ns (FWHM).

4. 2-D calculation using "Atlant" code have been performed to study thin-shell target implosion stability and spontaneous magnetic field generation. Fig.6a gives initial values for typical single-shell run:initial radius R_g° =225 μm (A_s=225) gas-fill-density ρ_g° =6.64.10^{-4}g/cm^3. Initial perturbations have the form $R_{1(2)} = R_{1(2)}^{\circ}(1 + \frac{\alpha\Delta}{R_{1(2)}^{\circ}} \cos n\vartheta)$ where $\Delta = (R_1^{\circ} - R_2^{\circ})$, α, is relative amplitude of perturbation, $(R_1^{\circ} - R_2^{\circ})$ is initial shell thickness.

Fig.6b presents target shell shape at the moment of maximum gas compression. In this run we have studied perturbation having har -

monic number n=50 and initial amplitude α =0.05. It is seen that relative perturbations have grown considerably in the nonevaporated part of the target. Thermal flux from the gas to the shell leads to evaporation of inner boundary layers in the shell (see Fig.).This effect has led to a significant smoothing of perturbation due to thermal conduction. The pure hydrodynamic run (thermal conduction cancelled) led to larger shell distortions.

The calculational results are in good agreement with high-aspect ratio target experimental results on the "Delphin" installation. /3/ .Similar results were given in paper /10/. Typical computational results are: average ion temperature of compressed gas is 1.5 keV, minimal gas radius R_{min}=16-18 μm, neutron yield is $1.6.10^8$.

In the same target but for pure spherical case (without any perturbations) the average ion temperature amounts to 1.7 keV, R_{min}= =16 μm, neutron yield is 3.10^8.

In earlier computational investigations of implosion stability of relatively low-aspect ratio shells /7/ ($A_s \sim 30-50$) at laser pulse energy E_{las}=10-50 J the stabilization of perturbation growth rate due to thermal flux from gas to shell was not found.

Next calculation series investigated implosion stability of double-shell targets. Double-shell target as compared to a single -shell target gives a possibility to obtain higher energy concentration in the target centre due to essential increase of the inner shell velocity after the collision with the external one /8/.Initial conditions for typical double-shell run are as follows: external SiO_2 shell radius R_g^o =280 um and aspect ratio $A_s^{(1)}$=140, inner polyethylene shell - R_s^o =91 um, $A_s^{(2)}$=91, gas density in the central cavity and between the shells is ρ_g^o =10^{-3} g/cm^3 (see Fig.7a). It was

assumed that the external shell had spherical symmetry and the inner one had shell shape perturbations with relative initial amplitude α =0.05 and harmonic number n=10. Due to heat conduction stabi - lization the inner shell was not destroyed at the moment of maximal gas compression in spite of sufficiently high initial perturbation amplitude.

Spontaneous magnetic field generation during target implosion was investigated using 2-D numerical simulations.

Crossed temperature and density gradients occur due to growth of hydrodynamic perturbations. This well known effect leads to spontaneous magnetic fields generation by thermocurrent mechanism:

$$\frac{\partial B}{\partial t} \sim \frac{c}{e} \nabla T \times \nabla \ln \rho + \dots$$

The field growth becomes very large during shell decoeleration /9/. In the calculations presented the magnetic field reached up 30 MG in double shell target. In such field the $\chi = \omega_B \cdot \tau_e$ parameter (for DT-plasma with ion temperature T =4.5 keV and density ρ = =2.1 g/cm^3) is ~10. So, the radial thermal flux is partially suppressed. This effect leads to some increase in the central gas temperature as compared to the calculations when magnetic field generation is cancelled.

References

1. Afanasiev Yu.V., Gamaly E.G., Gus'kov S.Yu., Rozanov V.B. Analytical theory and scaling for thin shell target implosion. FIAN Preprint N30, 1980.
2. Basov N.G., Volosevich P.P., Gamaly E.G. et al. JETP, 1980, v.78, p.420-429.
3. Basov N.G., Galichy A.A., Ganilov A. et al. JETP Letts., 1983, v.37,
4. Kasenjar S., Skupsky S., Entenberg A., Goldman L., Richardson M. Phys.Rev.Lett., 49, 7, 463 (1982).
5. Volosevich P.P., Bogtyarev L.M., Levanov E.I. et al. Fizika plazmy 1976, v.2, N6, p.883.
6. Samarsky A.A., Gaifulin S.A., Zakharov A.V. et al. Problemy atomnoi nauki i tekhniki. Ser.: Methods and codes for numerical solution of mathematical physics problems, 1982, 2-d issue .
7. Gamaly E.G., Rozanov V.B., Samarsky A.A., Tishkin N.M., Favorsky A.P. JETP, 1979, v.979, p.459-472.
8. Basov N.G., Gamaly E.G., Gus'kov S.Yu., Rozanov V.B., Kvantovaya Elektronika, 1982, v.9, N10, p.1945-1954.
9. Gamaly E.G., Gasilov V.A., Lebo I.G., Rozanov V.B. Trudy FIAN. v.134, M., Nauka, 1982, p.84-98.
10. Bokov N.N., Bunatian A.A., Likov V.A., et al. JETP Pisma, 1977, v.26, N9, p.630-634.

TARGET

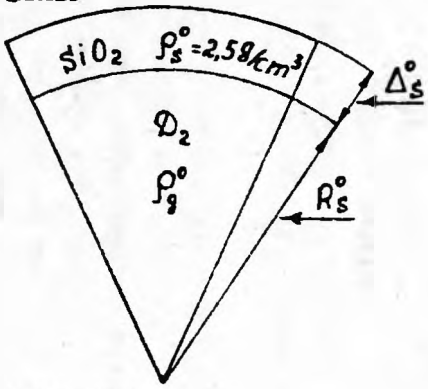

LASER PULSE

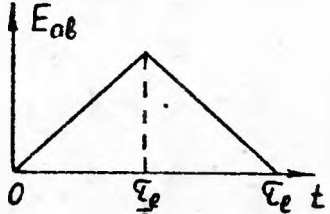

DIANA

CALCULATIONS

$R_s^o = 250\mu$, 200μ

$\Delta = 0{,}5\mu \div 5\mu$

$A_s = \frac{R_s^o}{\Delta_s^o} = 50 \div 400$

$E_{ol} = 400 J$, $\tau_l = 4{,}4$ ns

LUCH

CALCULATIONS

$R_s^o = 70\mu$

$\Delta = 1\mu$, 2μ

$E_{ol} = 20 \div 50 J$

$\tau_l = 2{,}5$ ns

$$q = \frac{E_{ol}}{4\pi R_s^{o2} \tau_l} = 1{,}8 \cdot 10^{13}, 1{,}2 \cdot 10^{13} \frac{W}{cm^2}$$

SOME EXPLONATIONS TO SYMBOLS

ρ_{cr} PLASMA CRITICAL DENSITY

M_s^o, M_g SHELL AND GAS MASS

$\mathcal{I}$. COEFFICIENT OF THE TRANSFER OF SHELL HYDRODYNAMIC ENERGY TO THE GAS THERMAL ENERGY.

γ ADIABATIC EXPONENT

Fig 1

MAXIMUM SHELL VELOCITY

SCALING

$$u_s^* = \left(\frac{12}{5}\right)^{1/2} \left(\frac{R_s^\circ}{\Delta_s^\circ} \cdot \frac{\rho_{cr}}{\rho_s^\circ}\right)^{1/2} \left[\frac{2(\gamma-1)}{3\gamma-1} \cdot \frac{q}{\rho_{cr}}\right]^{1/2}; \quad A_s = \frac{R_s^\circ}{\Delta_s^\circ}, \quad q = \frac{E_{ab}}{4\pi R_s^{\circ 2} t_\ell}$$

$$u_s^* \sim A_s^{1/2} q^{1/3}$$

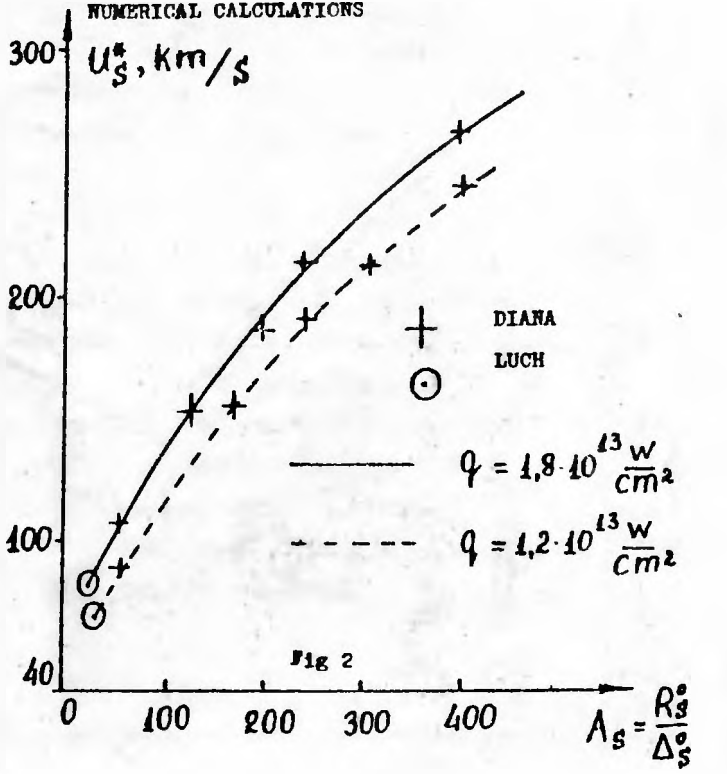

Fig 2

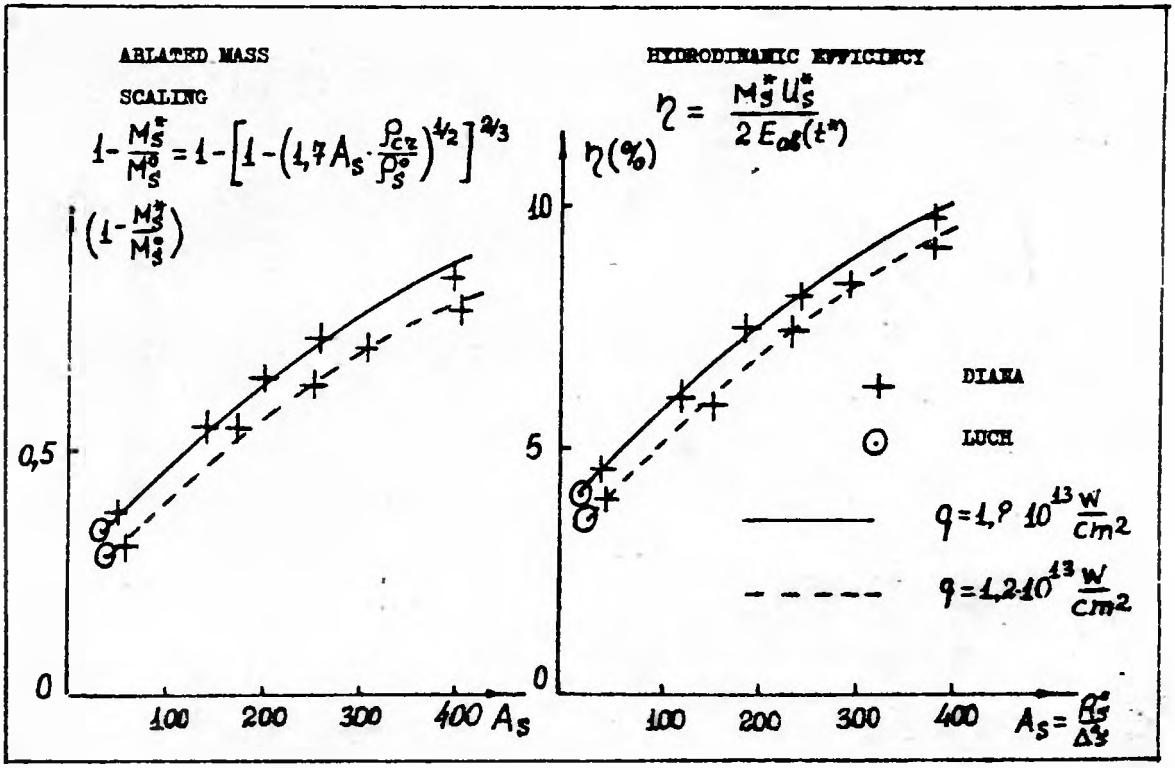
ABLATED MASS
SCALING
$1-\frac{M_s^*}{M_s^0}=1-\left[1-\left(1{,}7A_s\cdot\frac{\rho_{cr}}{\rho_s^0}\right)^{1/2}\right]^{2/3}$
$\left(1-\frac{M_s^*}{M_s^0}\right)$
0,5
0
100
200
300
400
A_s
HYDRODINAMIC EFFICIENCY
$\eta=\frac{M_s^* U_s^*}{2E_{as}(t^*)}$
$\eta(\%)$
10
5
0
DIANA
LUCH
$q=1{,}9\ 10^{13}\frac{W}{cm2}$
$q=1{,}2\ 10^{13}\frac{W}{cm2}$
100
200
300
400
$A_s=\frac{\rho_s^0}{\Delta s}$

Fig 3

FINAL DEUTERIUM PLASMA TEMPERATURE

$$T_g^* = \frac{1}{2} U_s^* \frac{M_s^*}{M_g} \cdot \chi \quad ; \quad \chi = \frac{\mathcal{E}_{i.g.}}{\mathcal{E}_{kin.s.}} = \left[1 + \frac{M_s^*}{M_g} \left(\frac{\rho_g^o}{\rho_s^o} \right)^{\frac{\gamma-1}{3}} a^{-\frac{1}{3}} \right]^{-1}$$

SCALING:

$$T_g^* \sim q^{2/3} \left(\frac{\rho_s^o}{\rho_g^o} \right) \left[\frac{A_s}{A_s + 3 \left(\frac{\rho_s^o}{\rho_g^o} \right)^{1/3} a^{-1/3}} \right] \cdot \frac{M_s^*}{M_s^o}$$

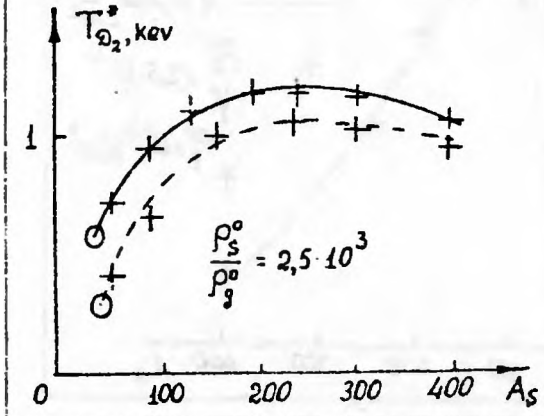

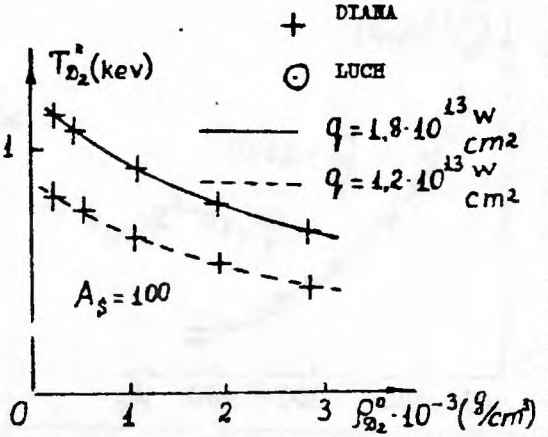

Fig 4

FINAL DEUTERIUM PLASMA DENSITY

SCALING

$$\rho_g^* = 4\left(\frac{\gamma+1}{\gamma-1}\right)\rho_g^0\left(\frac{M_s^*}{M_g}\chi\right)^{\frac{1}{\gamma-1}}$$

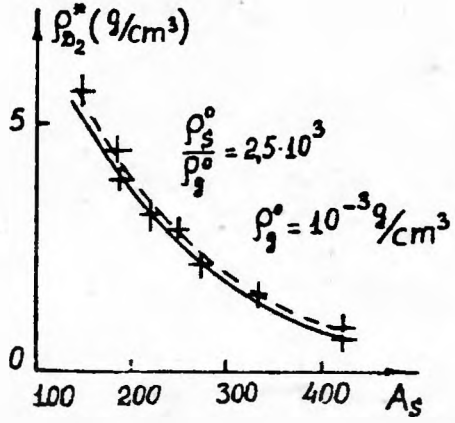

NEUTRON YIELD

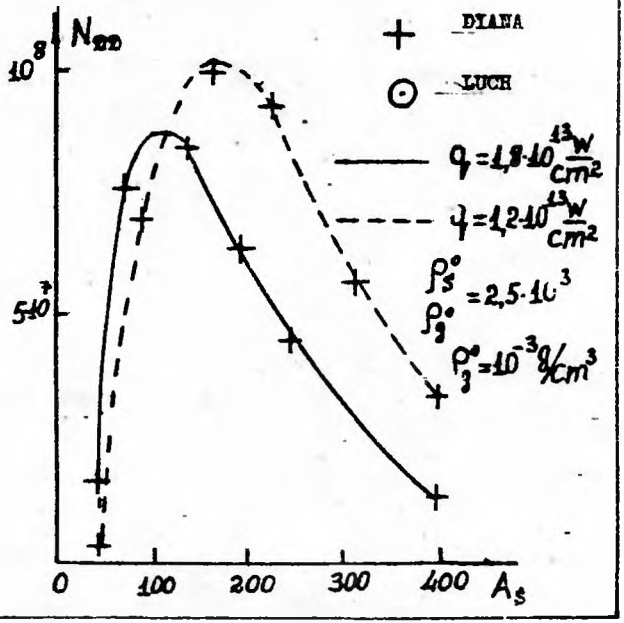

Fig 5

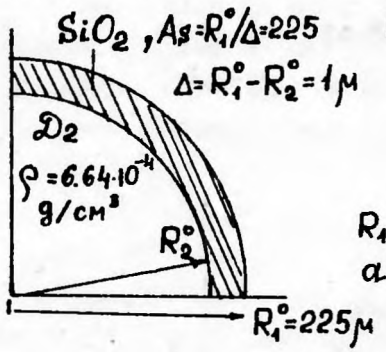
SiO_2, $A_s = R_1^\circ/\Delta = 225$
$\Delta = R_1^\circ - R_2^\circ = 1\mu$
D_2
$\rho = 6.64 \cdot 10^{-4}$ g/cm³
R_2°
$R_1^\circ = 225\mu$
$\dot{E}_L$
$E_L = 360$ J
0.8
3.1
4.1
t ns
$R_{1(2)} = R_{1(2)}^\circ \left(1 + \frac{a \cdot \Delta}{R_{1(2)}^\circ} \cos n\vartheta\right)$
$a = 0.05$, $n = 50$

Fig 6 A

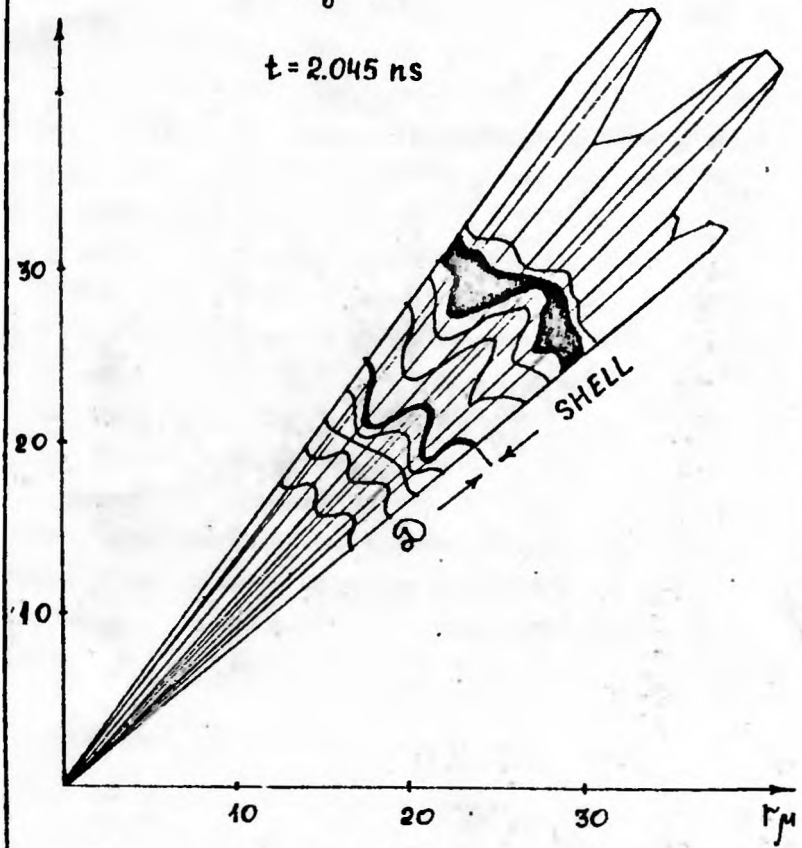
t = 2.045 ns
30
20
10
SHELL
ρ
10
20
30
r μ

Fig 6 B

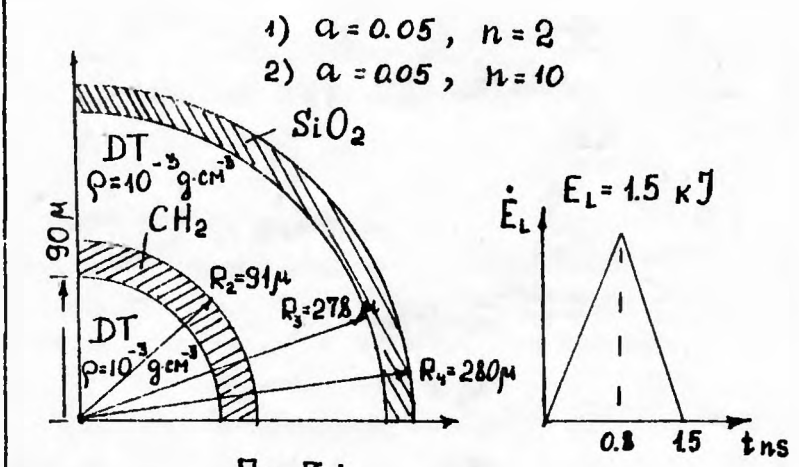
1) a = 0.05 , n = 2
2) a = 0.05 , n = 10
SiO2
DT
ρ=10^-3 g·cm^-3
CH2
90 μ
R2=91μ
R3=278
DT
ρ=10^-3 g·cm^-3
R4=280μ
Ė_L
E_L = 1.5 kJ
0.8
1.5
t ns

Fig 7A

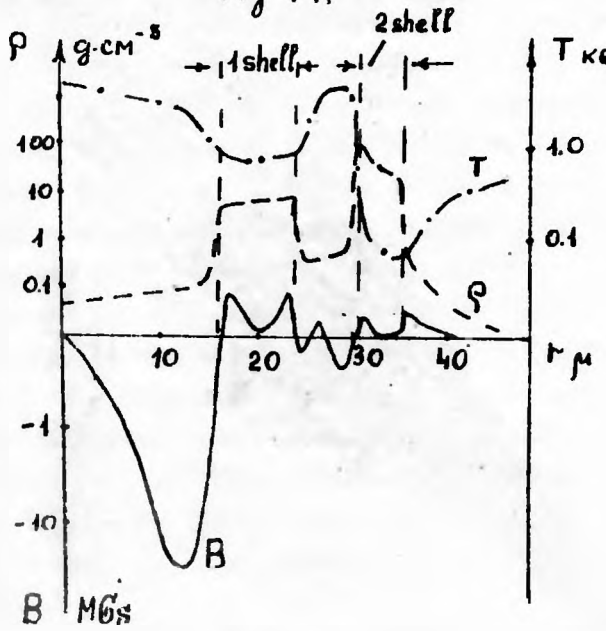
ρ g·cm^-3
1 shell
2 shell
T keV
100
10
1
0.1
1.0
0.1
T
ρ
10
20
30
40
r μ
-1
-10
B
B MGs

Fig 7B

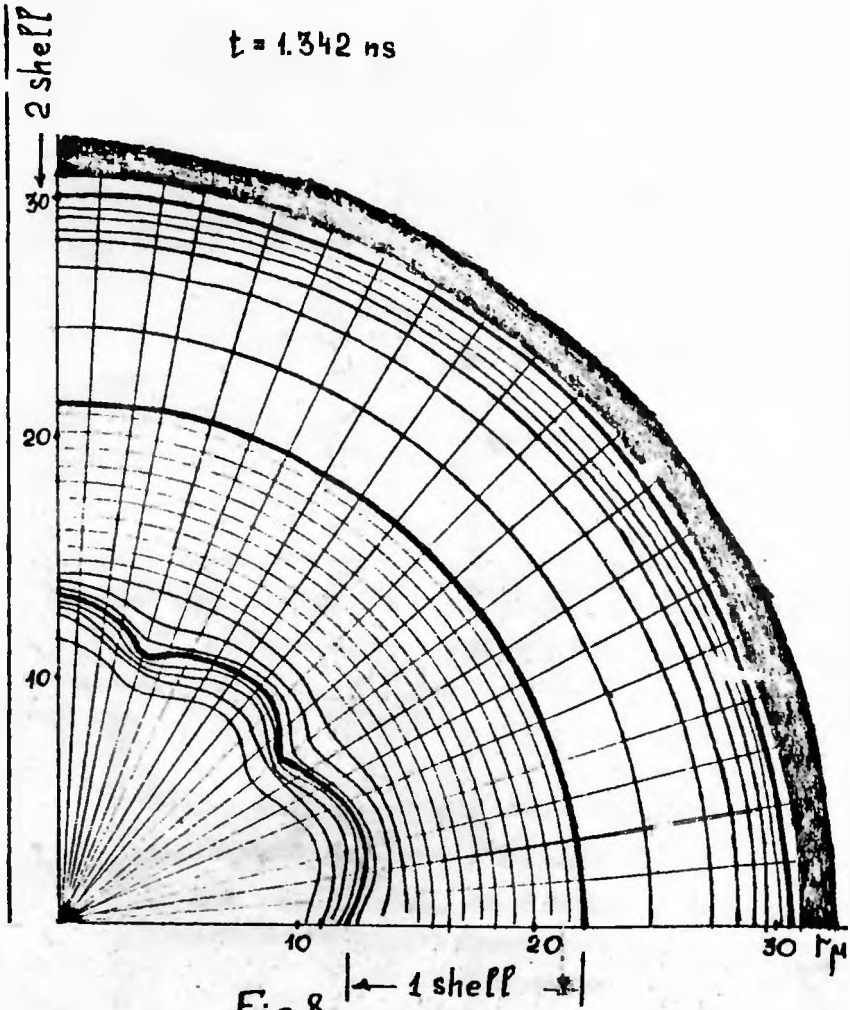

Fig 8